Supplementary Information for:

Chemical characterization and formation of secondary organosiloxane aerosol (SOSiA) from OH oxidation of decamethylcyclopentasiloxane

Yanfang Chen[a,b], Yoojin Park[c], Hyun Gu Kang[d], Jiwoo Jeong[a], Hwajin Kim[a,b*]

[a]Department of Environmental Health Sciences, Graduate School of Public Health, Seoul National University, 08826 Seoul, South Korea

[b]Institute of Health and Environment, Graduate School of Public Health, Seoul National University, 08826 Seoul, South Korea

[c]Department of Environmental Science and Engineering, College of Engineering, Ewha Womans University, 03760 Seoul, South Korea

[d]Multiphase Chemistry Department, Max Planck Institute for Chemistry, 55128 Mainz, Germany

For Environ. Sci.: Atmos

This file includes:

8 Pages

10 Figures

3 Tables

References

Table S1. Summary of PAM-OFR experiments.

Experiment ID	AMS	Filter	RH (%)	T (°C)	$[H_2O]$ (%)	$[D_5]_{init}$ (ppb)	$[D_5]_{final}$ (ppb)	OH_{exp} (molec. sec. cm^{-3})	Aging Day
1	√		27.76	26.57	0.953			3.85×10^{11}	2.97
2		√	29.82	20.37	0.704	245.16	135.20	6.57×10^{10}	0.51
3		√	29.43	20.78	0.713	231.86	119.29	1.21×10^{11}	0.94
4		√	29.14	21.02	0.716	224.62	101.46	1.92×10^{11}	1.48
5		√	28.35	23.03	0.788	225.94	88.00	3.53×10^{11}	2.72
6		√	31.35	23.54	0.899	222.53	80.61	4.04×10^{11}	3.12
7		√	80.64	22.12	2.12	229.37	108.80	2.09×10^{11}	1.61
8		√	79.44	23.35	2.25	228.39	83.81	2.72×10^{11}	2.1
9		√	76.07	24.02	2.24	186.98	67.94	4.54×10^{11}	3.5
10		√	72.21	24.73	2.22	222.48	56.32	8.24×10^{11}	6.36
11		√	73.59	24.15	2.19	241.04	56.39	9.12×10^{11}	7.04

Additional notes for AMS measurement: we've performed a series of experiments with AMS measurement, however, the AMS fragments could not provide the molecular composition or the formation mechanisms of SOSiA. Thus, only the representative AMS mass spectra was used in our study. The RH and temperature were averaged values monitored in the PAM chamber with light on. $[D_5]_{init}$ and $[D_5]_{final}$ are the D_5 concentrations measured by PTR-MS before and after the reaction.

Table S2. D_5-SOSiA fragments measured by AMS.

Formula	Nominal Mass	Exact Mass
$C_2H_7Si^+$	59	59.0317
$C_3H_9Si^+$	73	73.0474
$C_3H_9O_2Si_2^+$	133	133.0141
$C_5H_{15}OSi_2^+$	147	147.0661
$C_5H_{15}O_2Si_2^+$	163	163.0611
$C_4H_{11}O_3Si_3^+$	191	191.0016
$C_3H_9O_4Si_3^+$	193	192.9809
$C_5H_{15}O_3Si_3^+$	207	207.0329
$C_4H_{13}O_4Si_3^+$	209	209.0122
$C_7H_{21}O_2Si_3^+$	221	221.0849
$C_7H_{21}O_3Si_3^+$	237	237.0798
$C_6H_{19}O_4Si_3^+$	239	239.0591
$C_4H_{11}O_5Si_4^+$	251	250.9684
$C_6H_{17}O_4Si_4^+$	265	265.0204
$C_5H_{15}O_5Si_4^+$	267	266.9997
$C_7H_{21}O_4Si_4^+$	281	281.0517
$C_9H_{27}O_3Si_4^+$	295	295.1037
$C_6H_{17}O_6Si_5^+$	325	324.9871
$C_5H_{15}O_7Si_5^+$	327	326.9664
$C_4H_{13}O_8Si_5^+$	329	328.9457
$C_7H_{21}O_6Si_5^+$	341	341.0184
$C_6H_{19}O_7Si_5^+$	343	342.9977
$C_9H_{27}O_5Si_5^+$	355	355.0705
$C_8H_{25}O_6Si_5^+$	357	357.0498
$C_{11}H_{33}O_4Si_5^+$	369	369.1225
$C_6H_{17}O_8Si_6^+$	385	384.9539
$C_7H_{21}O_8Si_6^+$	401	400.9852
$C_9H_{27}O_7Si_6^+$	415	415.0372
$C_{11}H_{33}O_6Si_6^+$	429	429.0893
$C_7H_{21}O_{10}Si_7^+$	461	460.9520
$C_9H_{27}O_9Si_7^+$	475	475.0040

Table S3. Identified molecular composition of D_5-SOSiA detected by ESI-MS ("D" refers to the units of $(CH_3)_2SiO$ and "T" refers to CH_3SiO.).

No.	Formula	Monoisotopic mass	Ion mode	Note
1	$C_3H_{10}O_3Si_2$	150.0169	$[M-H]^-$	DT-OH
2	$C_5H_{16}O_4Si_3$	224.0356	$[M-H]^-$	D_2T-OH
3	$C_4H_{14}O_5Si_3$	226.0149	$[M-H]^-$	$DT_2-(OH)_2$
4	$C_5H_{16}O_6Si_4$	284.0024	$[M-H]^-$	
5	$C_4H_{14}O_7Si_4$	285.9817	$[M-H]^-$	
6	$C_7H_{22}O_5Si_4$	298.0544	$[M-H]^-$	D_3T-OH
7	$C_6H_{20}O_6Si_4$	300.0337	$[M-H]^-$	$D_2T_2-(OH)_2$
8	$C_5H_{16}O_8Si_5$	343.9692	$[M-H]^-$	
9	$C_7H_{22}O_7Si_5$	358.0212	$[M-H]^-$	$D_3T-OH-SiO_2$
10	$C_6H_{20}O_8Si_5$	360.0005	$[M-H]^-$	$D_2T_2-(OH)_2-SiO_2$
11	$C_7H_{22}O_8Si_5$	374.0161	$[M-H]^-$	$D_2T_2-OH-CH_2OH-SiO_2$
12	$C_8H_{26}O_7Si_5$	374.0525	$[M+Na]^+$	$D_3T_2-(OH)_2$
13	$C_7H_{24}O_8Si_5$	376.0318	$[M+Na]^+$	$D_2T_3-(OH)_3$
14	$C_6H_{22}O_9Si_5$	378.0110	$[M-H]^-$	$DT_4-(OH)_4$
15	$C_8H_{26}O_8Si_5$	390.0474	$[M+Na]^+$	$D_2T_3-(OH)_2-CH_2OH$
16	$C_7H_{24}O_9Si_5$	392.0267	$[M+Na]^+$	$DT_4-(OH)_3-CH_2OH$
17	$C_9H_{28}O_9Si_5$	420.0580	$[M+Na]^+$	$DT_4-OH-(CH_2OH)_3$
18	$C_9H_{28}O_8Si_6$	432.0400	$[M-H]^-$	
19	$C_8H_{26}O_9Si_6$	434.0192	$[M-H]^-$	
20	$C_7H_{22}O_{11}Si_7$	477.9547	$[M-H]^-$	
21	$C_9H_{28}O_{10}Si_7$	492.0067	$[M-H]^-$	
22	$C_8H_{26}O_{11}Si_7$	493.9860	$[M-H]^-$	
23	$C_{10}H_{32}O_{10}Si_7$	508.0380	$[M-H]^-$	
24	$C_9H_{28}O_{12}Si_8$	551.9735	$[M-H]^-$	
25	$C_{11}H_{34}O_{11}Si_8$	566.0255	$[M-H]^-$	
26	$C_{10}H_{32}O_{12}Si_8$	568.0048	$[M-H]^-$	
27	$C_9H_{28}O_{14}Si_9$	611.9402	$[M-H]^-$	
28	$C_{11}H_{34}O_{13}Si_9$	625.9923	$[M-H]^-$	
29	$C_{12}H_{38}O_{13}Si_9$	642.0236	$[M-H]^-$	
30	$C_{11}H_{34}O_{15}Si_{10}$	685.9590	$[M-H]^-$	
31	$C_{13}H_{40}O_{14}Si_{10}$	700.0111	$[M-H]^-$	
32	$C_9H_{38}O_{19}Si_9$	701.9931	$[M-H]^-$	
33	$C_{14}H_{44}O_{14}Si_{10}$	716.0424	$[M-H]^-$	
34	$C_{13}H_{42}O_{15}Si_{10}$	718.0216	$[M-H]^-$	
35	$C_{13}H_{44}O_{16}Si_{10}$	736.0322	$[M-H]^-$	

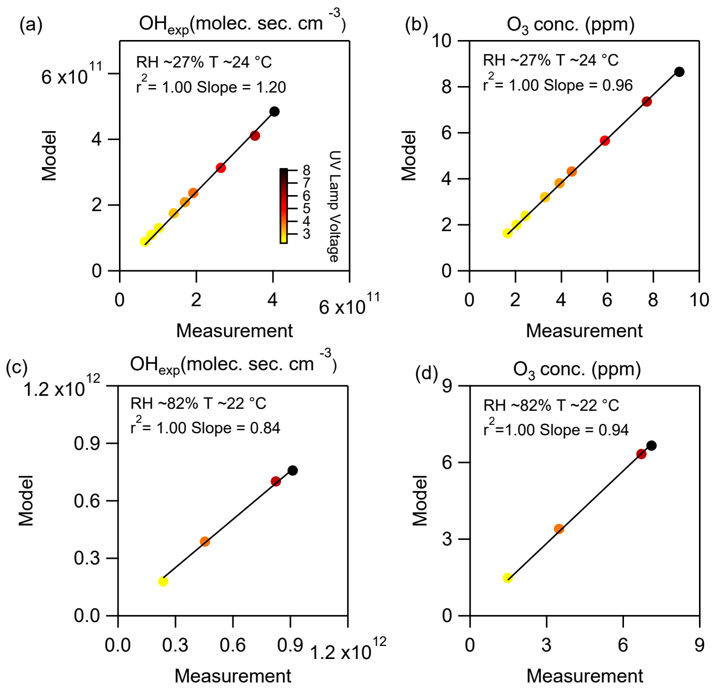

Figure S1. Comparison between modeled and measurement results for OH_{exp} (a and c) and O_3 mixing ratios (b and d) across different offline OH_{exp} calibration experiments. The modeled results were calculated from the KinSim chemical kinetic solver (4.6.1)[1] with the OFR185 mechanism from Rowe et al.[2]

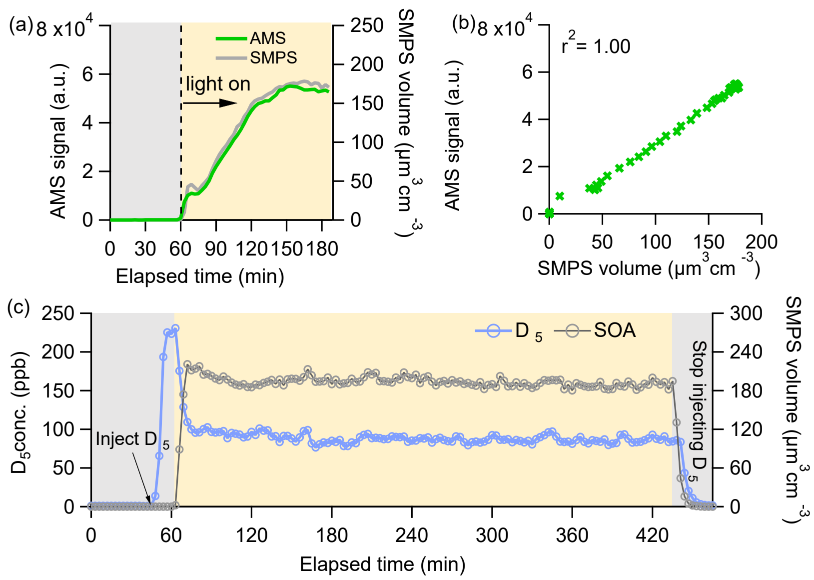

Figure S2. (a) Time evolution and (b) scatterplot of SOSiA measured by AMS and SMPS during experiment 1. (c) Time series of D_5 measured by PTR-MS and SMPS volume concentration during a representative filter collection experiment. The grey area indicates PAM-OFR light off period and light yellow is the light on period. Unfortunately, the PTR-MS was not available during the experiment 1. The fluctuation of the time series at the beginning is probably due to the unstable injection of D_5.

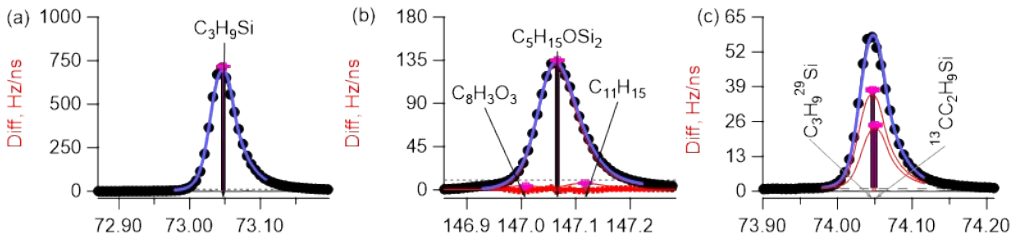

Figure S3. AMS high-resolution mass spectra of Si-containing fragments at (a) m/z 73, (b) m/z 147 and (c) m/z 74.

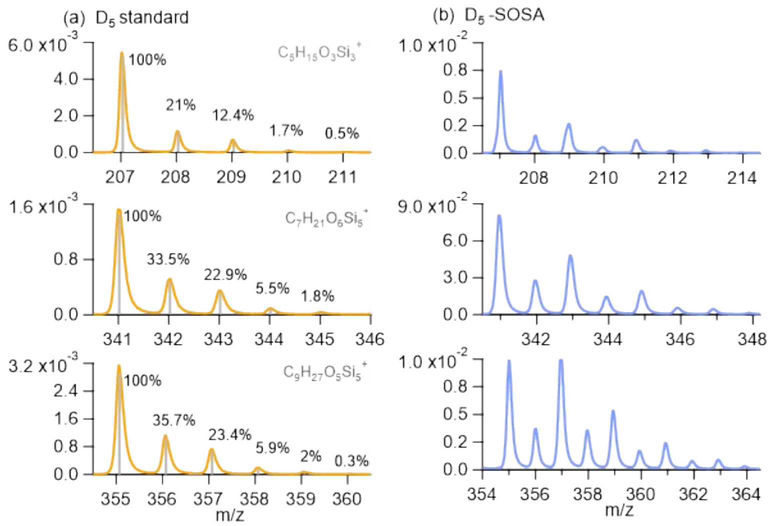

Figure S4. Raw mass spectra of (a) D_5 standard and (b) D_5-SOSiA detected with AMS. The height of vertical grey lines corresponds to the expected isotopic ratios.

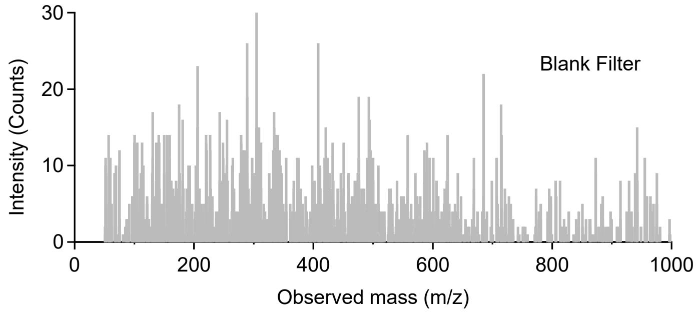

Figure S5. ESI-MS (-) mass spectrum of blank filter.

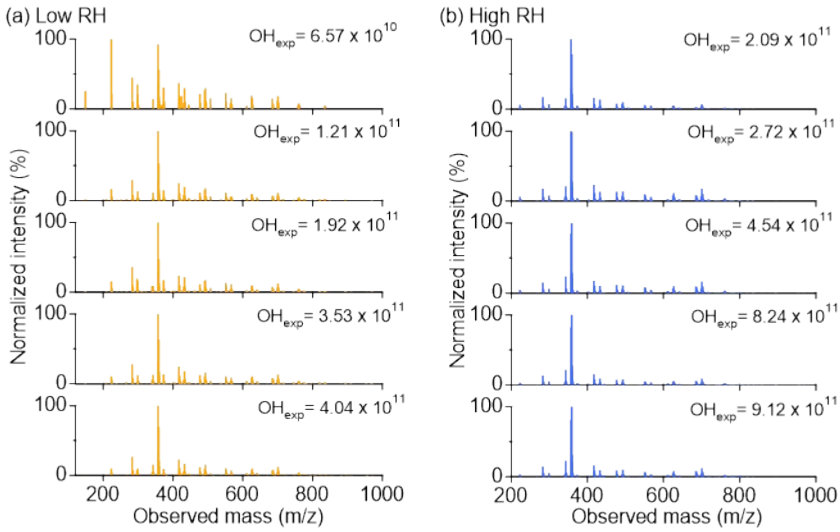

Figure S6. ESI-MS (-) mass spectrum of D_5-SOSiA at different OH exposure. The peak intensities are normalized by setting the abundance of the largest peak in each spectrum to 100.

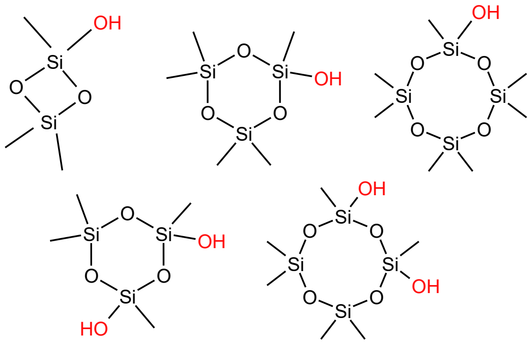

Figure S7. Possible structures of identified small silanols (DT-OH, D_2T-OH and D_3T-OH) and siloxandiols (DT_2-$(OH)_2$and D_2T_2-$(OH)_2$).

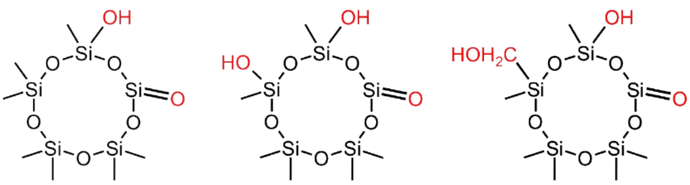

Figure S8. Possible structures of ring opening products (D_3T-OH-SiO_2, D_2T_2-$(OH)_2$-SiO_2 and D_2T_2-OH-CH_2OH-SiO_2).

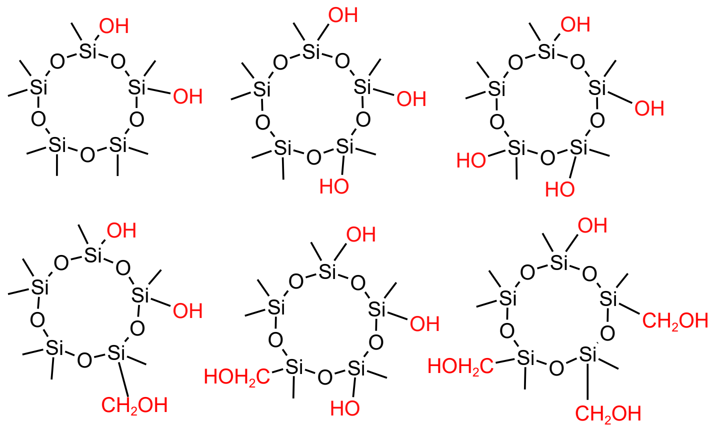

Figure S9. Possible structures of identified monomers (D_3T_2-$(OH)_2$, D_2T_3-$(OH)_3$, DT_4-$(OH)_4$, D_2T_3-$(OH)_2$-CH_2OH, DT_4-$(OH)_3$-CH_2OH and DT_4-OH-$(CH_2OH)_3$).

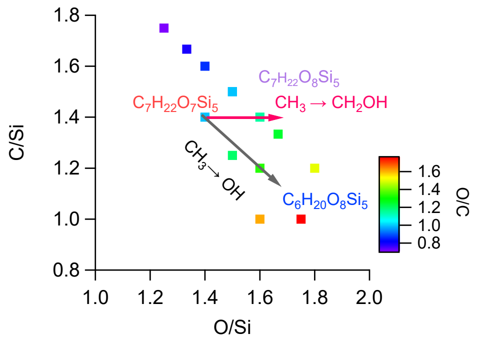

Figure S10. Plots of C/Si versus O/Si for ring-opening SOSiA products between m/z 200-400.

References

1. Z. Peng and J. L. Jimenez, KinSim: A Research-Grade, User-Friendly, Visual Kinetics Simulator for Chemical-Kinetics and Environmental-Chemistry Teaching, *Journal of Chemical Education*, 2019, **96**, 806-811.

2. J. P. Rowe, A. T. Lambe and W. H. Brune, Technical Note: Effect of varying the λ = 185 and 254 nm photon flux ratio on radical generation in oxidation flow reactors, *Atmos. Chem. Phys.*, 2020, **20**, 13417-13424.